HHS Public Access

Author manuscript

J Allergy Clin Immunol. Author manuscript; available in PMC 2020 August 01.

Published in final edited form as:

J Allergy Clin Immunol. 2019 August ; 144(2): 574–583.e5. doi:10.1016/j.jaci.2019.03.002.

Immunodeficiency and Epstein Barr virus induced lymphoproliferation caused by 4-1BB deficiency

Mohammed Alosaimi, M.D.[a,b], **Manfred Hoenig, M.D**[c], **Faris Jaber, M.D**[a], **Craig D. Platt, M.D, Ph.D.**[a], **Jennifer Jones, B.A**[a], **Jacqueline Wallace, B.S.P.H**[a], **Klaus-Michael Debatin, M.D.**[c], **Ansgar Schulz, M.D.**[c], **Eva Jacobsen, Ph.D.**[c], **Peter Möller, M.D.**[d], **Hanan E. Shamseldin, M.Sc.**[e], **Ferdous Abdulwahab, M.Sc.**[e], **Niema Ibrahim, M.D.**[e], **Hosam Alardati, M.D.**[f], **Faisal Almuhizi, M.D.**[g], **Ibraheem F. Abosoudah, M.D.**[h], **Talal A. Basha, M.D.**[i], **Janet Chou, M.D.**[a,#], **Fowzan S. Alkuraya, M.D.**[e,#], **Raif S. Geha, M.D.**[a,#]

[a]Division of Immunology, Boston Children's Hospital and Department of Pediatrics Harvard Medical School, Boston, MA, USA

[b]Department of Pediatrics, King Saud University, Riyadh, Saudi Arabia

[c]Department of Pediatrics and Adolescent Medicine University Medical Center Ulm, Germany

[d]Institute of Pathology University of Ulm, Germany

[e]Department of Genetics, King Faisal Specialist Hospital and Research Center, Riyadh, Saudi Arabia

[f]Department of Pathology and Laboratory Medicine, King Faisal Specialist Hospital and Research Center, Jeddah, Saudi Arabia

[g]Department of Medicine, Security Force Hospital, Riyadh, Saudi Arabia

[h]Department of Oncology, King Faisal Specialist Hospital and Research Center, Jeddah, Saudi Arabia

[i]Department of Pediatrics, King Faisal Specialist Hospital and Research Center, Jeddah, Saudi Arabia

Abstract

Background: The tumor necrosis family factor receptor (TNFR) family member 4-1BB (CD137) is encoded by *TNFRSF9* and expressed on activated T cells. 4-1BB provides a co-stimulatory signal that enhances $CD8^+$ T cell survival, cytotoxicity, and mitochondrial activity, thereby promoting immunity against viruses and tumors. The ligand for 4-1BB (4-1BBL) is expressed on antigen-presenting cells and Epstein-Barr virus (EBV) transformed B cells.

Corresponding author: Raif S. Geha, Division of Immunology, Boston Children's Hospital, 1 Blackfan Circle, Karp Building 10th floor, Boston, MA, 02115, USA. Tel: (617) 919-2482; Fax: (617) 730-0528; raif.geha@childrens.harvard.edu.
[#]Equal contribution

Conflict of interest: The authors declare no conflicts of interest.

Objective: We investigated the genetic basis of recurrent sino-pulmonary infections, persistent EBV viremia, and EBV-induced lymphoproliferation in two unrelated patients.

Methods: Whole exome sequencing, immunoblotting, immunophenotyping, and *in vitro* assays of lymphocyte and mitochondrial function were performed.

Results: The two patients shared a homozygous G109S missense mutation in 4-1BB that abolished protein expression and ligand binding. The patients' $CD8^+$ T cells had reduced proliferation, impaired expression of interferon-γ (IFN-γ) and perforin, and diminished cytotoxicity against allogeneic and HLA matched EBV-B cells. Mitochondrial biogenesis, membrane potential, and function were significantly reduced in the patients' activated T cells. An inhibitory antibody against 4-1BB recapitulated the patients' defective $CD8^+$ T cell activation and cytotoxicity against EBV-infected B cells *in vitro.*

Conclusion: This novel immunodeficiency demonstrates the critical role of 4-1BB co-stimulation in host immunity against EBV infection.

Capsule summary:

We have identified a novel immunodeficiency associated with EBV induced lymphoproliferation due to a homozygous missense mutation in 4-1BB, demonstrating a critical role for 4-1BB in the human immune response against EBV-driven B cell lymphoproliferation.

Keywords

4-1BB; CD137; immunodeficiency; Epstein-Barr virus; Hodgkin lymphoma

INTRODUCTION

EBV is a common infectious pathogen with a strong tropism for B lymphocytes[1]. In immunocompetent hosts, primary EBV infection is often asymptomatic, or a self-limited disease. In contrast, a subset of immunodeficient patients are susceptible to persistent EBV viremia associated with fever, lymphadenopathy, hepatitis, and pneumonia[2]. Complications of EBV infection in immunodeficient patients include uncontrolled B cell proliferation, hemophagocytic lymphohistiocytosis (HLH), and malignancies[2].

EBV-specific immunity depends on virus-specific cellular and humoral immunity. The importance of $CD8^+$ cytotoxic T cells in the control of EBV infection is demonstrated by the susceptibility of patients with mutations in genes critical for T cell development and function to chronic EBV infection[3]. These include defects in genes associated with severe combined immunodeficiencies, *MAGT1,* a Mg^{+2} transporter involved in TCR and NKG2D signaling, *SH2D1A,* which encodes the SLAM-associated protein SAP, *ITK,* which encodes IL-2-inducible T cell kinase, and *PFR1* which encodes perforin 1[4]. Mutations in the T cell co-stimulatory TNF family member receptor CD27 and its ligand, the TNFR family member CD70 predominantly expressed on B cells, result in impaired generation of IFN-γ and perforin-producing $CD8^+$ cytotoxic T cells[5, 6]. T cell activation and EBV-specific $CD8^+$ T cell expansion and cytotoxicity are impaired in CD70-deficient patients[7, 8].

4-1BB is a Type II transmembrane protein of the TNFR family expressed as a trimer on the surface of activated T cells[9]. 4-1BB has four cysteine-rich domain (CRDs) in its extracellular region, of which the CRD2 and CRD3 domains comprise the ligand-binding domain. The intracellular region of 4-1BB interacts with TNFR associated factor 2 (TRAF2)[10]. The ligand for 4-1BB, 4-1BBL (CD137L), is a member of the TNF family expressed as a trimer on the surface of activated T cells, B cells, dendritic cells (DCs), and natural killer (NK) cells[11-14]. Notably, the EBV encoded latent membrane protein 1 (LMP1) upregulates 4-1BBL expression on B cells[15]. 4-1BB ligation enhances the activation of both human $CD4^+$ and $CD8^+$ T cells, but preferentially promotes the expansion and increased survival of $CD8^+$ T cells. Activation of 4-1BB enhances the production of IFN-γ and perforin and mitochondrial biogenesis, contributing to the cytolytic activity of $CD8^+$ T cells[16-20]. The contribution of 4-1BB to $CD8^+$ T cell function is further demonstrated by the decreased IFN-γ production and cytolytic $CD8^+$ T cell effector function in 4-1BB-deficient mice[21]. The effect of 4-1BB stimulation on cytolytic T cell responses has been used to increase the potency of vaccines against cancers[22, 23]. Additionally, incorporation of the intracellular domain of 4-1BB in the architecture of chimeric antigen receptors (CARs) increases the cytotoxicity of CAR T cells against tumor targets[24, 25].

We present two unrelated patients with sinopulmonary infections, chronic EBV viremia, and EBV-driven lymphoproliferation. The patients shared a homozygous G109S missense mutation in 4-1BB that abolished 4-1BB surface expression and ligand binding. The patients' $CD8^+$ T cells demonstrated reduced proliferation, impaired expression of interferon-γ (IFN-γ) and perforin, and diminished cytotoxicity against allogeneic and HLA-matched EBV-transformed B cells. Addition of an inhibitory 4-1BB antibody to cultures of normal PBMCs stimulated with allogeneic or autologous EBV-B cells recapitulated the patients' $CD8^+$ T cell functional defects. These results support a critical role for 4-1BB in host immunity against EBV infection.

MATERIALS AND METHODS

Patients.

All study participants provided written informed consent approved by the respective institutional review boards of the referring hospitals.

Genetic studies.

Genomic DNA was genotyped using genomewide SNP array (Axiom SNP chip). The genotype files were analyzed using AutoSNPa software (http://dna.leeds.ac.uk/autosnpa/) to search for shared regions of homozygosity (ROH) followed by in-depth analysis of the underlying haplotypes. Exome sequencing was performed as described before[26]. Variants were prioritized based on residing within the candidate autozygous interval, being coding/splicing variants and being novel or very rare (MAF<0.0001) in public databases (gnomAD) and our database of 2379 ethnically matched in-house exomes as described [27]. Sanger sequencing was used to validate the identified mutation in the probands and verify the carrier status of the parents.

Immunophenotyping.

The conjugated monoclonal antibodies used for flow cytometry studies of T and B cells were: anti-CD45RA APC-CY7, anti-CD56 PE, anti-CD3 FITC, anti-CD4 BV605, anti-CD8 APC and anti-CCR7 Bv421, all from BioLegend.

T cell proliferation.

T cell proliferation was measured by adding 1 μCi of [^{3}H]thymidine for 16 h after stimulation with immobilized anti-CD3 (3 μg/mL) (OKT3, eBioscience) and anti-CD28 (1 μg/mL) (eBioscience) or PHA (4 μg/mL) (Sigma Aldrich) as previously described[28].

Cytokine secretion.

Interferon-γ (INF-γ) and IL-2 were measured in supernatants of PHA stimulated PBMCs using a cytometric bead array (CBA) from BD Biosciences according to the manufacturer's instructions.

4-1BB and 4-1BBL expression and 4-1BBL binding.

Five × 10^5 unstimulated and PHA (4 μg/mL) stimulated PBMCs were stained on ice for 30 min with anti-4-1BB PE, anti-4-1BBL APC, anti-CD4 BV605, anti-CD8 FITC and anti-CD25 BV421, all from BioLegend. For 4-1BBL binding, PBMCs were incubated first with chimeric CD137L:muCD8 fusion protein (Axxora ANC-503) then washed and incubated with murine anti-CD8 PE.

Immunoblotting.

Lysates from PHA (4 μg/mL) stimulated PBMCs in RIPA buffer (Millipore) and protease inhibitors (Sigma-Aldrich offers Roche) were electrophoresed on 4-12% precast polyacrylamide gels (Bio-Rad), followed by immunoblotting with polyclonal rabbit antibody against the intracellular region of 4-1BB (LS-C135872). Anti-β-actin antibody was used as control (Cell Signaling).

Intracellular cytokine staining.

Five × 10^5 PBMCs were incubated with PMA (5 ng/ml), ionomycin (500 ng/ml), Brefeldin A and Monensin for 4 hours then fixed and permeabilized with BD Cytofix/Cytoperm. Cells were then incubated overnight on ice with anti-IFN-γ-APC, anti-Perforin-PE and anti-CD8 FITC all from bioLegend. Analyses were performed using the FlowJo software.

Cytotoxic T cell generation and killing assay.

EBV-transformed B cell line were generated as described[29]. PBMCs were stimulated with Mitomycin C treated autologous or allogeneic EBV-LCL in the presence of IL-7 (10 ng/mL) (PeproTech). 4-1BB blocking antibody (LifeSpan BioScienes; clone BBK-2-azide free) was added every 7 days to control PBMCs cultures. Three rounds of stimulation were performed at 7-day intervals. IL-2 (100 U/mL) was added on day 14 of culture. A responder to stimulator ratio of 10:1 was used throughout the rounds of stimulation. At day 21, $CD8^+$ T cells were isolated by negative selection using the $CD8^+$ T Cell Isolation Kit from Miltenyi Biotec as per the manufacturer's protocol. $CD8^+$ T cells were incubated for 4 hrs with live

EBV-B cell targets at different effector to target [E:T] cell ratios and cytotoxicity was measured by flow cytometry gating on $CD19^+$ and using Annexin V and fixable viability dye (FVD) (Thermo Fisher Scientific) as described[30]. Cytotoxicity percentage was measured as 100 minus the percentage of Annexin-V and FVD negative EBV-cells.

Oxygen consumption.

Oxygen consumption rates (OCR) was measured by Seahorse XFp Analyzer. 1×10^5 T lymphocytes, which were purified form PHA stimulated PBMCs cultures for 3 days, were plated per each well in Seahorse XF base media with 2 mM Glutamine, 10 mM Glucose and 2.5 mM Pyruvate. OCR was measured at baseline and in the presence of 1 uM oligomycin, 4 uM CCCP and 0.5 uM antimycin A/ rotenone.

Mitochondrial studies.

Unstimulated and PHA (4ug/mL) stimulated 5×10^5 PBMCs were stained at 37°C for 25 minuts with MitoTracker Green (100nM) and MitoTracker Red CMXRos (200nM). Cells were washed with warm phosphate buffered saline and immediately analyzed without fixation. Mitochondrial stains were from Thermo Fisher.

Statistics.

Statistical analysis was performed using GraphPad Prism. Student's t test was used for comparisons of two groups; unless otherwise indicated, one-way ANOVA was used for the comparison of more than 2 groups, with the Holm-Ćídák post-comparison test. Data are graphed as mean with SEM.

RESULTS

Two patients with immunodeficiency and EBV lymphoproliferation.

We studied two Saudi patients, products of first cousin marriages, but not known to be related. Patient 1 (P1) presented at 3 years of age with sinopulmonary infections, bronchiectasis, and an episode of pneumococcal septicemia. Her sinopulmonary infections improved with intravenous gammaglobulin (IVIG) replacement therapy. At 5 years of age, she developed generalized lymphadenopathy and was found to have EBV viremia (Fig. 1A). Cervical lymph node (LN) biopsy showed multiple clusters of $CD20^+$ B cells (Fig. 1B). *In situ* hybridization was positive for EBV-encoded RNA (Fig. 1B). Laboratory evaluation at that time revealed normal numbers of T, B and natural killer cells, hypogammaglobulinemia (IgG 440 mg/dL, normal range 500-1,490 mg/dL; IgM 318 mg/dL, normal range 37-224 mg/dL; IgA <45 mg/dL, normal range 29-256 mg/dL), poor antibody response to tetanus toxoid (TT) (0.2 IU/ml, normal range >0.4 IU/mL) and undetectable antibody titres to pneumococcal polysaccharide vaccine (Pnumovax-23) which the patient has received (normal range >3.3 ug/mL) . She subsequently developed HLH with persistent fevers, splenomegaly, pancytopenia, elevated serum levels of triglycerides (345 mg/dL, normal <150 mg/dL), and soluble CD25 (>5000 pg/mL, normal 450-1997 pg/mL), and low serum fibrinogen (140 mg/dL, normal > 150 mg/dL). She was treated with anti-CD20 mAb (rituximab), leading to resolution of her viremia (Fig. 1A). Post Rituximab treatment, she was found to have increased percentages of T effector memory cells, undetectable B cells,

and decreased proliferation to phytohemagglutinin (PHA) and anti-CD3+anti-CD28 stimulation (Table 1). PHA-driven IFN-γ secretion by PBMCs was significantly reduced, but IL-2 secretion was normal (Fig. 1C). She is currently undergoing hematopoietic stem cell transplantation (HSCT) from a healthy HLA-matched sibling.

Patient 2 (P2) presented at six years of age with recurrent sinopulmonary infections, generalized lymphadenopathy, splenomegaly, and EBV viremia (Fig. 1D). He had elevated serum levels of IgG (4898 mg/dL, normal range 34-274 mg/dL) and IgA (272 mg/dL, normal range 25-154 mg/dL), but low levels of IgM (25 mg/dL, normal range 38-251 mg/dL). He was diagnosed with EBV-positive Hodgkin's disease. He received five cycles of chemotherapy in the form of doxorubicin, bleomycin, vincristine, etoposide, prednisone and cyclophosphamide (ABVE-PC) along with rituximab. Chemotherapy and rituximab treatment resulted in clinical remission and resolution of the viremia. IVIG replacement therapy improved his respiratory infections. Subsequently, he was found to have decreased numbers of T cells with increased percentages of T effector memory cells, undetectable B cells, and reduced proliferation to PHA and anti-CD3+anti-CD28 stimulation. PHA-driven IFN-γ secretion by PBMCs was significantly reduced, but IL-2 secretion was normal (Fig. 1F), as observed in Patient 1. He relapsed one year later with recurrence of lymphoma and EBV viremia (Fig. 1D). LN biopsy showed a progression to a diffuse large B cell lymphoma (DLBCL) negative for CD20 and positive for CD38 expression (Fig 1E). *In situ* hybridization was positive for EBV-encoded RNA (Fig. 1E). He received daratumumab (anti-CD34 mAb)., bortezomib, dexamethasone and rituximab (anti-CD20 mAb). This resulted in clinical improvement and resolution of the viremia. P2 has no HLA-matched siblings.

A homozygous 4-1BB^{G109S} mutation in the patients abolishes 4-1BB expression.

Homozygosity analysis of SNP array results revealed that the two patients shared one region of homozygosity (ROH) that comprised an identical founder haplotype: Chr1:7186325-8273940 (delimited by SNPs rs4460663-rs395847). Although the patients' families are not known to be related, the shared interval suggests a founder effect. Whole exome sequencing revealed only two novel homozygous variants within this candidate locus, *CAMTA1* and *TNFRSF9.* The *CAMTA1* variant (NM_015215.3:c.2370C>G: p.Ile790Met) affected a poorly conserved residue and was considered unlikely since the gene has an established link to autosomal dominant cerebellar ataxia with mental retardation, a phenotype irrelevant to the patient. The shared *TNFRSF9* variant (NM_001561:c.325G>A: p.Gly109Ser), was absent in gnomAD and in our database of 2379 ethnically matched in-house exomes. The *TNFRSF9* variant was predicted to be pathogenic by PolyPhen (0.999), SIFT (0.03), and CADD (30). Sanger sequencing revealed that the mutation is homozygous in both patients (Fig. 2A), and heterozygous in their parents (data not shown). Table E1 lists all the variants shared by both probands with a minor allelic frequency (MAF) of <0.001 in gnomAD. No exonic mutations in any of the genes known to be associated with immunodeficiency and EBV-driven B cell lymphoproliferation were detected

The mutated G109 residue in 4-1BB is highly conserved (Fig. 2B). It resides in the third CRD of the extracellular region of 4-1BB, but does not directly interact with the 4-1BB

ligand, 4-1BBL (Fig. 2C,D). Modeling based on the crystal structure of the 4-1BB/4-1BBL complex[9] suggests that the mutated S109 residue could form hydrogen bonds with nearby polar residues, altering the protein's folding, structure, or stability (Fig. 2D).

4-1BB is expressed on T cells only after activation[17]. Immunoblotting using a polyclonal rabbit antibody directed against the intracellular domain of 4-1BB (residues 214-255) revealed 4-1BB expression in lysates from PHA-activated PBMCs from healthy controls, but not from the two patients (Fig. 2E), indicating that the mutant protein is not expressed. PHA stimulation induced 4-1BB surface expression on $CD8^+$ and $CD4^+$ cells from controls, but not from the two patients (Fig. 2F and S1A). Furthermore, recombinant 4-1BBL bound PHA-activated $CD8^+$ and $CD4^+$ T cells from controls, but not from the patients (Fig. 2E and S1A). The absence of 4-1BB expression and 4-1BBL binding by the patient T cells was not secondary to poor T cell activation, as the patients' $CD8^+$ and $CD4^+$ T cells robustly upregulated CD25 surface expression following PHA activation (Fig. 2E and S1A). Consistent with lack of expression of the mutant protein, PHA-activated $CD4^+$ and $CD8^+$ T cells from the heterozygous parents of the patients demonstrated a ~ 50% reduction in 4-1BB expression (Fig. S1B).

Defective expansion, reduced expression of IFN-γ and perforin, and impaired allo- and EBV-specific cytotoxic activity of patient $CD8^+$ T cells.

4-1BB co-stimulation promotes $CD8^+$ T cell expansion, IFN-γ and perforin secretion, and cytotoxic activity[16-18, 31]. To determine the impact of the $4\text{-}1BB^{G109S}$ mutation on the generation and function of cytotoxic $CD8^+$ T cells, PBMCs were stimulated in three consecutive one week rounds with mitomycin-C treated allogeneic EBV B cells from a non-HLA matched donor (Fig. 3A). In these co-cultures, EBV-B cells express 4-1BBL and activated $CD8^+$ T cells express 4-1BB (Fig. S2). After the second and third rounds of stimulation (Days 14 and 21), aliquots of cells were analyzed for $CD8^+$ T cell numbers and intracellular expression of IFN-γ and perforin (Fig. 3A). Stimulation with allogeneic EBV-B cells caused progressive expansion and intracellular expression of IFN-γ and perforin in control $CD8^+$ T cells (Fig. 3B, C). In contrast, the patients' $CD8^+$ T cells had significantly less expansion compared to controls and reduced expression of IFN-γ and perforin (Fig. 3B, C). After three rounds of stimulation, control $CD8^+$ T cells purified from normal cultured PBMCs stimulated with allogeneic EBV cells exhibited robust cytotoxicity against the priming EBV-B cells (Fig. 3D). As expected, they had minimal cytotoxicity against EBV-B cells from a third party donor, HLA-mismatched with the donor of the EBV-B cell line used for stimulation (<5% killing at E:T cell ratio of 8:1), demonstrating the specificity of EBV-primed cytotoxic $CD8^+$ T cells to the priming donor cells. The cytotoxic activity of the patients' $CD8^+$ T cells against allogeneic EBV-B cells was significantly reduced compared to that of control $CD8^+$ T cells from healthy controls (Fig. 3D). Importantly, addition of an inhibitory anti-4-1BB antibody to cultures of normal PBMCs stimulated with allogeneic EBV-B cells reduced the expansion, intracellular expression of IFN-γ and perforin, and allo-cytotoxicity to levels comparable to those of the patients' $CD8^+$ cells (Fig. 3B-D). Collectively, these findings demonstrate that 4-1BB deficiency impairs the generation and function of allo-cytotoxic $CD8^+$ cells.

EBV-specific $CD8^+$ cell cytotoxicity is important for EBV immunity and is typically tested using autologous EBV-B cells[2, 8]. We were unable to generate EBV-transformed B cell lines from the patients since both had undetectable B cells after Rituximab treatment. In lieu of this, we tested the EBV-specific expansion and cytotoxicity of $CD8^+$ cells in cultures of PBMCs from P1 against EBV-transformed B cells from her HLA-matched sibling. The expansion and cytotoxicity of $CD8^+$ cells in cultures of PBMCs from a control donor stimulated with autologous EBV-B cells were used as a positive control. The stimulation protocol was similar to the one used to test cytotoxicity against allogeneic EBV-B cells (Fig. 3A). Priming of normal PBMCs with autologous EBV-B cells caused $CD8^+$ T cells to expand, express IFN-γ and perforin, and exhibit cytotoxicity against autologous EBV-B cell targets (Fig. 3E-G), but not against autologous PHA T cell blasts (<5% killing at E:T cell ratio of 8:1). $CD8^+$ T cells expansion, expression of IFN-γ and perforin, and cytotoxicity against HLA-matched EBV-B cell targets were significantly reduced in cultures of PBMCs from P1 stimulated with HLA-matched EBV-B cells compared to control cultures stimulated with autologous EBV-B cells (Fig. 3E-G). Addition of an inhibitory anti-4-1BB antibody reduced the cytotoxicity of control $CD8^+$ cells against autologous EBV-B cells to a level comparable to that of patient $CD8^+$ cells against HLA-matched EBV-B cells (Fig. 3E-G). Collectively, these data support a critical role for 4-1BB in the expansion and function of EBV-specific $CD8^+$ cells.

Defective mitochondrial biogenesis and function in the patients' activated T cells.

In PHA-stimulated PBMC cultures, $CD19^+$ B cells, $CD14^+$ monocytes and $CD11c^+$ dendritic cells express 4-1BBL that interacts with 4-1BB expressed on activated T cells (Fig. S3). 4-1BB ligation enhances mitochondrial biogenesis and increases oxidative phosphorylation in activated T cells[19, 20]. We used extracellular flux analysis to measure the oxygen consumption rate (OCR) in T cells purified from PHA-stimulated PBMC cultures. The combination of protons, electrons, and oxygen in the mitochondrial matrix determines the mitochondrial oxygen consumption rate and reflects mitochondrial function. In the inner mitochondrial membrane, Complexes I – IV of the electron transport chain catalyze electron transfers and generate the proton gradient across the inner mitochondrial membrane that ultimately drives ATP synthesis by Complex V. The addition of oligomycin (Olig) to purified T cells inhibits proton flow through Complex V, revealing the basal OCR generated by Complexes I-IV (Fig. 4A). FCCP (carbonyl cyanide-4(trifluoromethoxy) phenylhydrazone) permeabilizes the inner mitochondrial membrane, permitting proton entry into the mitochondrial matrix through the concentration gradient, thereby providing the substrate for maximal OCR (Fig. 4A). Rotenone and antimycin inhibit Complexes I and III, thereby terminating electron transport chain function and abrogating mitochondrial respiration (Fig. 4A). P2 T cells showed decreased basal and maximal oxygen consumption (Fig. 4B), indicating reduced mitochondrial function activity compared to controls. Similarly, the addition of an inhibitor anti-4-1BB antibody to PHA-stimulated control PBMCs reduced the baseline and maximal OCR to a level comparable to that of patient T cells (Fig. 4B).

To further delineate the mechanisms underlying the impaired mitochondrial function in the patients' T cells, we measured mitochondrial mass and membrane potential in PHA-

activated $CD8^+$ T cells. The mitochondrial mass in the patients' activated $CD8^+$ T cells was significantly reduced compared to that of controls (Fig. 4C). The mitochondrial membrane potential, which is determined by the electric polarization of the inner mitochondrial membrane, is required for oxidative phosphorylation, mitochondrial structure, and function. The mitochondrial membrane potential of the patients' activated $CD8^+$ T cells was significantly reduced compared to that of controls (Fig. 4D). Mitochondrial mass and membrane potential were also found to be significantly reduced in PHA-activated $CD4^+$ patient T cells (Fig. S4). Together, these results indicate that 4-1BB deficiency impairs mitochondrial biogenesis and function in activated T cells.

DISCUSSION

We report two patients with immunodeficiency and EBV-driven lymphoproliferation caused by a homozygous missense mutation in 4-1BB. 4-1BB protein was not detected on the surface of the patient's PHA-activated T cells by either flow cytometry or in their lysates by immunoblotting using a different antibody. Furthermore, the mutation abolished 4-1BBL binding to activated T cells from the patients. The patients' $CD8^+$ T cells had impaired expansion, reduced expression of IFN-γ and perforin, and defective cytotoxicity against allogeneic EBV cell targets, demonstrating the contribution of 4-1BB to host immunity against EBV.

Both patients had recurrent sinopulmonary infections that improved with gammaglobulin replacement therapy. Patient 1, on whom data was available prior to treatment with Rituximab, had hypogammaglobulinemia and a poor antibody response to tetanus vaccination on presentation. The poor antibody response to tetanus is consistent with the impaired antibody response of 4-1BB-deficient mice to the T cell dependent antigen keyhole limpet hemocyanin[21]. 4-1BB ligation is known to amplify $CD4^+$ T cell proliferation and cytokine secretion. PHA driven IFN-γ secretion was impaired in both patients, whereas IL-2 secretion was intact, suggesting a more stringent requirement for 4-1BB co-stimulation for INF-γ secretion by human T cells. The patients' $CD4^+$ T cells demonstrated impaired mitochondrial function, indicative of impaired metabolic fitness. Therefore, ligation of 4-1BB on $CD4^+$ helper T cells by 4-BBL expressed on antigen presenting cells and B cells may be important for the optimal response to T cell dependent antigens.

The mechanism behind the poor antibody response to Pneumovax observed in Patient 1 is unknown. In humans, CD137 signaling promotes B cell proliferation and survival, as well as secretion of TNF-α[32], both of which are important for the antibody response to the type II T independent (TI) antigen pneumococcus vaccine[33]. Impaired proliferation or/and insufficient TNF-α secretion by 4-1BB deficient B cells in response to type II T independent (TI) antigens may underlie the poor antibody response to Pneumovax in Patient 1.

Of critical relevance to the EBV viremia and EBV-driven lymphoproliferation, $CD8^+$ T cell expansion, expression of IFN-γ and perforin, and cytotoxicity against allogeneic EBV-B cells were all severely impaired in both patients. As an HLA-matched donor has been identified for Patient 1, we showed that these markers of $CD8^+$ T cell activation were also severely impaired against HLA-matched EBV-B cells. Importantly, the addition of 4-1BB

inhibitory antibody to normal PBMCs stimulated with allogeneic or autologous EBV-B cells reduced $CD8^+$ T cell expansion, expression of IFN-γ and perforin, and cytotoxicity to levels comparable to those in the patients, thus recapitulating the functional defects of the patient's $CD8^+$ T cells. These findings also replicate the defects in the expansion, IFN-γ production and function of allocytotoxic $CD8^+$ T cells from 4-1BB deficient mice[21].

Costimulatory molecules, such as CD28 and ICOS, have been shown to enhance mitochondrial respiration, biogenesis, and increased membrane potential[34]. Mitochondrial function is critical for the function of activated T cells[35]. Activated $CD8^+$ T cells from the patients showed decreased oxygen consumption, decreased mitochondrial mass and reduced membrane potential. These defects are consistent with the known contribution of 4-1BB stimulation in promoting mitochondrial respiration and biogenesis[20], and likely contribute to the defective cytotoxicity of the patients' $CD8^+$ T cells against allogeneic and HLA-matched EBV-B cell targets. This is relevant to the patients' inability in clearing EBV infections and the failure of Patient 2 to eliminate his EBV-triggered B cell lymphoma.

NK cells, like T cells, express 4-1BB upon their activation by incubation with their targets and cytokines (IL-2, IL-15, or IL-21)[36]. Also, like in T cells, 4-1BB signalling promotes proliferation and IFN-γ secretion by activated NK cells[12]. However, the effect of 4-1BB ligation on the cytotoxicity of activated NK cells is controversial, with some studies showing enhancement while others show inhibition[37-39]. Given the ethical limitations on repeated blood sampling from patients with complex medical disorders, future studies with additional patients will be needed to define the role of 4-1BB on NK cytotoxicity.

Although the two patients we studied from unrelated families, they shared a single ROH, suggesting a founder effect. *TNFRSF9* was the only one of the two genes in the shared ROH that had a novel variant and was predicted to be pathogenic. Furthermore, the $CD8^+$ T cell defects in both patients were similar to those in *Tnfrsf9*$^{-/-}$ mice. Together these findings implicate the lack of 4-1BB expression as the cause of the disease in our patients. Identification of different mutations in *TNFRSF9* in patients with EBV-driven lymphoproliferation will provide further support for a causative role of 4-1BB deficiency.

In summary, we have identified a novel immunodeficiency associated with EBV lymphoproliferation due to a homozygous mutation in 4-1BB. Our results indicate the clinical importance of 4-1BB in immune surveillance against infection with EBV and its complications.

Extended Data

Table E1.

Variants shared by both probands with a minor allelic frequency (MAF) of <0.001 in gnomAD

Chromosome	Position	Gene name	Zygosity	Variants
Chr2	133075726	ZNF806	Heterozygous	NM_001304449: c. 1187A>G:p.Glu396Gly
Chr2	133075904	ZNF806	Heterozygous	NM_001304449: c. 1366dupA:p.Asn456Lysfs*85

Chromosome	Position	Gene name	Zygosity	Variants
Chr3	42251580	TRAK1	Heterozygous	NM_001265608: c.2064_2066del:p.Glu698del
Chr9	140773612	CACNA1B	Heterozygous	NM_000718: c.390+1->ACGACACGGAGCCCTATTTCATCGGGATCTTTTGCTTCGAGGCAGGGA
Chr17	21318588	KCNJ12	Heterozygous	NM_021012: UTR5.c.−65C>G
Chr17	9000169	MUC16	Heterozygous	NM_024690: c.40588G>A:p.Gly13530Ser
Chr1	7998274	TNFRSF9	Homozygous	NM_001561: c.325G>A:p.Gly109Ser
Chr1	7724977	CAMTA1	Homozygous	NM_015215: c.2370C>G:p.Ile790Met

Supplementary Material

Refer to Web version on PubMed Central for supplementary material.

Acknowledgements.

We are grateful to the patients, the patients' families for their participation in this study. This study was funded by the Perkin Fund (RG and JC); NIH grants AI124101 AI139633 (RSG), and 5K08AI116979 (JC). We thank Dr. Klaus Schwarz for facilitating the study. We thank the Genotyping and Sequencing Core Facilities at KFSHRC for their technical help. This work was supported in part by King Salman Center for Disability Research and the Saudi Human Genome Program.

Supported by: 5K08AI116979-04 (J.C.), 1R01AI139633-01 (RSG) and the Perkin Fund (RSG)

Abbreviations:

CAR	Chimeric antigen receptor
CRD	Four cysteine-rich domain
EBV	Epstein-Barr virus
E:T	Effector to target
HLA	Human leukocyte antigen
HLH	Hemophagocytic lymphohistiocytosis
HSCT	Hematopoietic stem cell transplantation
IFN-γ	Interferon-γ
IL-2	Interleukin 2
IVIG	Intravenous gammaglobulin
LN	Lymph node
MFI	Mean fluorescence intensity
PBMCs	Peripheral blood mononuclear cells
ROH	Shared region of homozygosity

TNF	Tumor necrosis factor
TNFR	Tumor necrosis factor receptor
TRAF2	TNFR associated factor 2
TT	Tetanus toxoid

REFERENCES

1. Kurth J, Spieker T, Wustrow J, Strickler GJ, Hansmann LM, Rajewsky K, et al. EBV-infected B cells in infectious mononucleosis: viral strategies for spreading in the B cell compartment and establishing latency. Immunity 2000; 13:485–95. [PubMed: 11070167]
2. Latour S, Winter S. Inherited Immunodeficiencies With High Predisposition to Epstein-Barr Virus-Driven Lymphoproliferative Diseases. Front Immunol 2018; 9:1103. [PubMed: 29942301]
3. Palendira U, Rickinson AB. Primary immunodeficiencies and the control of Epstein-Barr virus infection. Ann N Y Acad Sci 2015; 1356:22–44. [PubMed: 26415106]
4. Katano H, Ali MA, Patera AC, Catalfamo M, Jaffe ES, Kimura H, et al. Chronic active Epstein-Barr virus infection associated with mutations in perforin that impair its maturation. Blood 2004; 103:1244–52. [PubMed: 14576041]
5. Yamada S, Shinozaki K, Agematsu K. Involvement of CD27/CD70 interactions in antigen-specific cytotoxic T-lymphocyte (CTL) activity by perforin-mediated cytotoxicity. Clin Exp Immunol 2002; 130:424–30. [PubMed: 12452832]
6. van Montfrans JM, Hoepelman AI, Otto S, van Gijn M, van de Corput L, de Weger RA, et al. CD27 deficiency is associated with combined immunodeficiency and persistent symptomatic EBV viremia. J Allergy Clin Immunol 2012; 129:787–93 e6. [PubMed: 22197273]
7. Izawa K, Martin E, Soudais C, Bruneau J, Boutboul D, Rodriguez R, et al. Inherited CD70 deficiency in humans reveals a critical role for the CD70-CD27 pathway in immunity to Epstein-Barr virus infection. J Exp Med 2017; 214:73–89. [PubMed: 28011863]
8. Abolhassani H, Edwards ES, Ikinciogullari A, Jing H, Borte S, Buggert M, et al. Combined immunodeficiency and Epstein-Barr virus-induced B cell malignancy in humans with inherited CD70 deficiency. J Exp Med 2017; 214:91–106. [PubMed: 28011864]
9. Bitra A, Doukov T, Croft M, Zajonc DM. Crystal structures of the human 4-1BB receptor bound to its ligand 4-1BBL reveal covalent receptor dimerization as a potential signaling amplifier. J Biol Chem 2018; 293:9958–69. [PubMed: 29720398]
10. Jang IK, Lee ZH, Kim YJ, Kim SH, Kwon BS. Human 4-1BB (CD137) signals are mediated by TRAF2 and activate nuclear factor-kappa B. Biochem Biophys Res Commun 1998; 242:613–20. [PubMed: 9464265]
11. Harfuddin Z, Kwajah S, Chong Nyi Sim A, Macary PA, Schwarz H. CD137L-stimulated dendritic cells are more potent than conventional dendritic cells at eliciting cytotoxic T-cell responses. Oncoimmunology 2013; 2:e26859. [PubMed: 24482752]
12. Wilcox RA, Tamada K, Strome SE, Chen L. Signaling through NK cell-associated CD137 promotes both helper function for CD8+ cytolytic T cells and responsiveness to IL-2 but not cytolytic activity. J Immunol 2002; 169:4230–6. [PubMed: 12370353]
13. Watts TH. TNF/TNFR family members in costimulation of T cell responses. Annu Rev Immunol 2005; 23:23–68. [PubMed: 15771565]
14. Stephan MT, Ponomarev V, Brentjens RJ, Chang AH, Dobrenkov KV, Heller G, et al. T cell-encoded CD80 and 4-1BBL induce auto- and transcostimulation, resulting in potent tumor rejection. Nat Med 2007; 13:1440–9. [PubMed: 18026115]
15. Choi IK, Wang Z, Ke Q, Hong M, Qian Y, Zhao X, et al. Signaling by the Epstein-Barr virus LMP1 protein induces potent cytotoxic CD4(+) and CD8(+) T cell responses. Proc Natl Acad Sci U S A 2018; 115:E686–E95. [PubMed: 29311309]

16. Laderach D, Movassagh M, Johnson A, Mittler RS, Galy A. 4-1BB co-stimulation enhances human CD8(+) T cell priming by augmenting the proliferation and survival of effector CD8(+) T cells. Int Immunol 2002; 14:1155–67. [PubMed: 12356681]
17. Shuford WW, Klussman K, Tritchler DD, Loo DT, Chalupny J, Siadak AW, et al. 4-1BB costimulatory signals preferentially induce CD8+ T cell proliferation and lead to the amplification in vivo of cytotoxic T cell responses. J Exp Med 1997; 186:47–55. [PubMed: 9206996]
18. Wen T, Bukczynski J, Watts TH. 4-1BB ligand-mediated costimulation of human T cells induces CD4 and CD8 T cell expansion, cytokine production, and the development of cytolytic effector function. J Immunol 2002; 168:4897–906. [PubMed: 11994439]
19. Menk AV, Scharping NE, Rivadeneira DB, Calderon MJ, Watson MJ, Dunstane D, et al. 4-1BB costimulation induces T cell mitochondrial function and biogenesis enabling cancer immunotherapeutic responses. J Exp Med 2018; 215:1091–100. [PubMed: 29511066]
20. Teijeira A, Labiano S, Garasa S, Etxeberria I, Santamaria E, Rouzaut A, et al. Mitochondrial Morphological and Functional Reprogramming Following CD137 (4-1BB) Costimulation. Cancer Immunol Res 2018; 6:798–811. [PubMed: 29678874]
21. Kwon BS, Hurtado JC, Lee ZH, Kwack KB, Seo SK, Choi BK, et al. Immune responses in 4-1BB (CD137)-deficient mice. J Immunol 2002; 168:5483–90. [PubMed: 12023342]
22. Bartkowiak T, Curran MA. 4-1BB Agonists: Multi-Potent Potentiators of Tumor Immunity. Front Oncol 2015; 5:117. [PubMed: 26106583]
23. Chester C, Ambulkar S, Kohrt HE. 4-1BB agonism: adding the accelerator to cancer immunotherapy. Cancer Immunol Immunother 2016; 65:1243–8. [PubMed: 27034234]
24. Chester C, Sanmamed MF, Wang J, Melero I. Immunotherapy targeting 4-1BB: mechanistic rationale, clinical results, and future strategies. Blood 2018; 131:49–57. [PubMed: 29118009]
25. Li G, Boucher JC, Kotani H, Park K, Zhang Y, Shrestha B, et al. 4-1BB enhancement of CAR T function requires NF-kappaB and TRAFs. JCI Insight 2018; 3.
26. Monies D, Abouelhoda M, AlSayed M, Alhassnan Z, Alotaibi M, Kayyali H, et al. The landscape of genetic diseases in Saudi Arabia based on the first 1000 diagnostic panels and exomes. Hum Genet 2017; 136:921–39. [PubMed: 28600779]
27. Alkuraya FS. Discovery of mutations for Mendelian disorders. Hum Genet 2016: 135:615–23. [PubMed: 27068822]
28. Jabara HH, Boyden SE, Chou J, Ramesh N, Massaad MJ, Benson H, et al. A missense mutation in TFRC, encoding transferrin receptor 1, causes combined immunodeficiency. Nat Genet 2016; 48:74–8. [PubMed: 26642240]
29. Hui-Yuen J, McAllister S, Koganti S, Hill E, Bhaduri-McIntosh S. Establishment of Epstein-Barr virus growth-transformed lymphoblastoid cell lines. J Vis Exp 2011.
30. Noto A, Ngauv P, Trautmann L. Cell-based flow cytometry assay to measure cytotoxic activity. J Vis Exp 2013:e51105. [PubMed: 24378436]
31. Chacon JA, Wu RC, Sukhumalchandra P, Molldrem JJ, Sarnaik A, Pilon-Thomas S, et al. Co-stimulation through 4-1BB/CD137 improves the expansion and function of CD8(+) melanoma tumor-infiltrating lymphocytes for adoptive T-cell therapy. PLoS One 2013; 8:e60031. [PubMed: 23560068]
32. Zhang X, Voskens CJ, Sallin M, Maniar A, Montes CL, Zhang Y, et al. CD137 promotes proliferation and survival of human B cells. J Immunol 2010; 184:787–95. [PubMed: 20008291]
33. Ryffel B, Di Padova F, Schreier MH, Le Hir M, Eugster HP, Quesniaux VF. Lack of type 2 T cell-independent B cell responses and defect in isotype switching in TNF-lymphotoxin alpha-deficient mice. J Immunol 1997; 158:2126–33. [PubMed: 9036957]
34. Klein Geltink RI, O'Sullivan D, Corrado M, Bremser A, Buck MD, Buescher JM, et al. Mitochondrial Priming by CD28. Cell 2017; 171:385–97.e11. [PubMed: 28919076]
35. Sena LA, Li S, Jairaman A, Prakriya M, Ezponda T, Hildeman DA, et al. Mitochondria are required for antigen-specific T cell activation through reactive oxygen species signaling. Immunity 2013; 38:225–36. [PubMed: 23415911]
36. Li X, He C, Liu C, Ma J, Ma P, Cui H, et al. Expansion of NK cells from PBMCs using immobilized 4-1BBL and interleukin-21. Int J Oncol 2015; 47:335–42. [PubMed: 25975533]

37. Vinay DS, Choi BK, Bae JS, Kim WY, Gebhardt BM, Kwon BS. CD137-deficient mice have reduced NK/NKT cell numbers and function, are resistant to lipopolysaccharide-induced shock syndromes, and have lower IL-4 responses. J Immunol 2004; 173:4218–29. [PubMed: 15356173]

38. Baessler T, Charton JE, Schmiedel BJ, Grunebach F, Krusch M, Wacker A, et al. CD137 ligand mediates opposite effects in human and mouse NK cells and impairs NK-cell reactivity against human acute myeloid leukemia cells. Blood 2010; 115:3058–69. [PubMed: 20008791]

39. Navabi S, Doroudchi M, Tashnizi AH, Habibagahi M. Natural Killer Cell Functional Activity After 4-1BB Costimulation. Inflammation 2015; 38:1181–90. [PubMed: 25520217]

Key messages:

- We identified a homozygous missense mutation in *TNFRSF9* encoding the T cell co-stimulatory molecule 4-1BB in two unrelated patients with recurrent infections, persistent Epstein Barr virus (EBV) viremia, and EBV-induced lymphoproliferation.
- The 4-1BB mutation abolished surface expression of 4-1BB on activated T cells.
- $CD8^+$ T cells from the patients had impaired proliferation, reduced expression of IFN-γ and perforin, and diminished cytotoxic activity in response to stimulation with allogeneic and HLA-matched EBV transformed B cells.
- Activated $CD8^+$ T cells from the patients had reduced mitochondrial mass, membrane potential, and function.

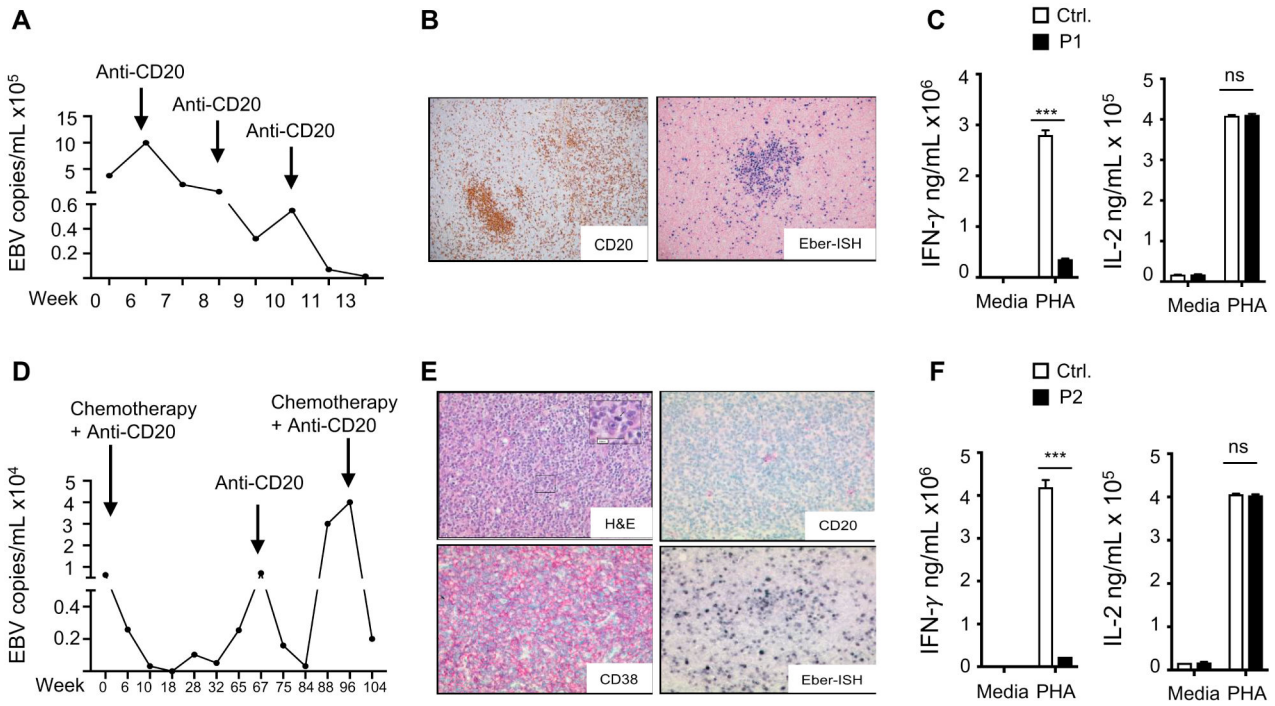

Figure 1. EBV viremia EBV driven lymphoproliferation and impaired IFN-γ secretion in the patients.

A. Circulating EBV viral load in P1. **B.** Immunohistochemistry of cervical LN from P1 showing a cluster of $CD20^+$ B cells (left) and positive EBV (EBER) *in situ* hybridization (right) **C.** IFN-γ and IL-2 levels in supernatants of PHA Stimulated PBMCs from P1 and controls (n=3) in two independent experiments. **D.** Circulating EBV viral load P2. **E.** H&E stain of cervical LN from P2 showing a diffuse growth pattern (upper left), and immunohistochemistry showing negative CD20 staining (upper right), positive CD38 staining (lower left) and positive EBV (EBER) in *situ* hybridization (lower right) consistent with a DLBCL of plasmablastic subtype. **F.** IFN-γ and IL-2 levels in supernatants of PHA Stimulated PBMCs from P2 and controls (n=3) in two independent experiments. Results represent the mean, columns and bars represent mean + SEM. *** $p<0.001$, ns= not significant.

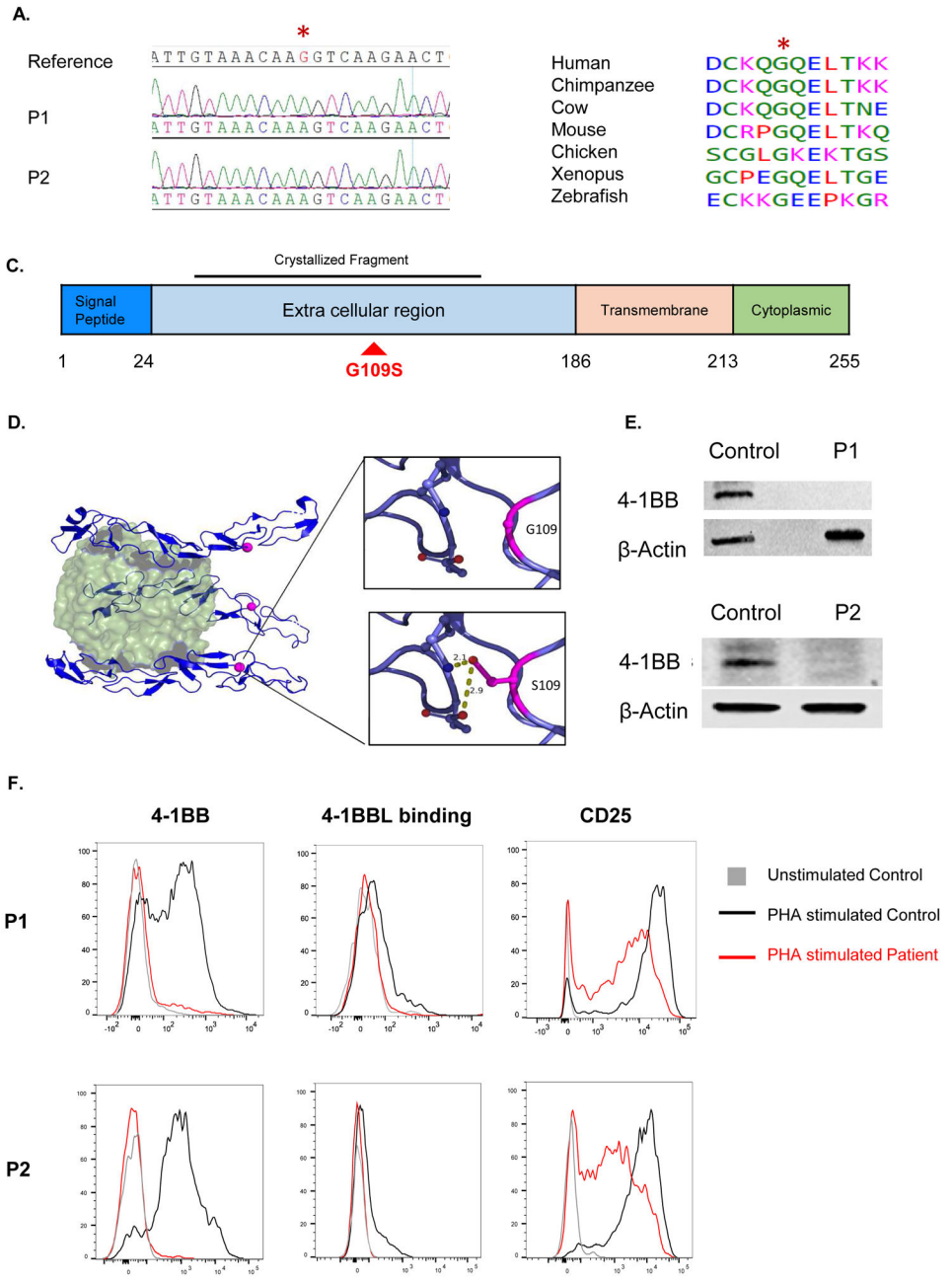

Figure 2. The 4-1BB^{G109S} mutation and its impact on 4-1BB expression.

A. Sanger sequencing around the missense *TNFRSF9* mutation (c.325G>A: p.Gly109Ser) in a reference control and patients. The mutated nucleotide is indicated in red and by an asterisk. **B.** Evolutionary conservation of the S109 a.a. in 4-1BB. Protein sequence orthologous to human 4-1BB was aligned in six non-human vertebrate species, all of which shared the p.S109 amino acid. **C.** Linear schematic of 4-1BB showing its domains and the location of the G109S mutation (red) in the extracellular domain. The 4-1BB fragment crystallized in complex with 4-1BB (PDB:6PCR) is indicated **D.** Ribbon diagram of the 4-1BB extracellular in complex 4-1BBL. The 4-1B trimer (blue) is shown bound to its trimeric ligand 4-1BBL (green). The red dot corresponds to the location of the mutated

G109 residue. The insets illustrate the potential of the mutated S109 residue to form hydrogen bonds with neighboring polar residues. **E.** Immunoblot analysis of PHA stimulated PBMCs from both patients and controls using a polyclonal antibody directed against the intracellular domain of 4-1BB. Actin was used as loading control. **F.** FACS analysis of 4-1BB expression (left), 4-1BBL binding (center) and CD25 expression(right) in PHA stimulated $CD8^+$ T cells from the patients and a control. Similar results were obtained from two independent experiments in E and F.

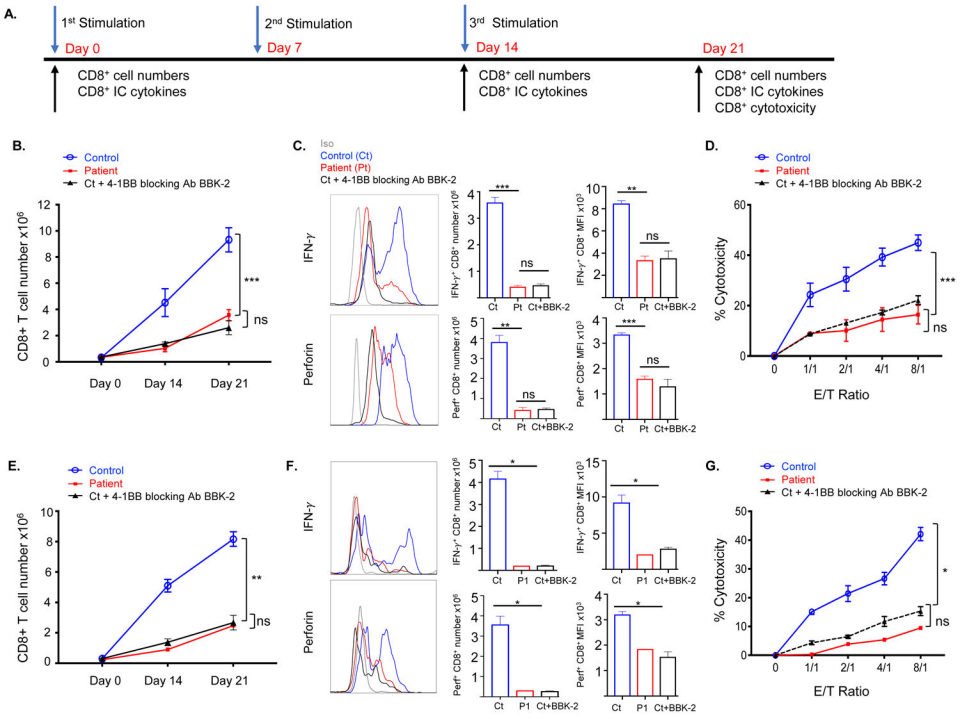

Figure 3. The 4-1BB^{G109S} mutation Impairs the generation of allo- and EBV-specific CD8$^+$ T cells.

A. Experimental protocol for the generation and testing of cytotoxic CD8$^+$ T cells against EBV-B cells. **B.** CD8$^+$ T cell numbers on days 0, 14 and day 21 post-stimulation with allogeneic EBV-B cells of PBMCs from patients (n=2) controls (n=4) and controls with addition of anti-4-1BB blocking antibody BBK-2 (n=2). **C.** Representative FACS analysis (left) quantitative analysis (center) and MFI (right) of CD8$^+$IFN-γ^+ and CD8$^+$Perforin$^+$ cells on Day 14 post stimulation of PBMCs stimulated with allogeneic EBV-B cells as described in B. **D.** Cytotoxic activity of CD8$^+$ T cells against the stimulatory allogeneic EBV B cells. CD8$^+$ T cells were purified on Day 21 from cultures of stimulated PBMCs from patients (n=2) controls (n=4). The effect of anti-4-1BB blocking antibody BBK-2 was examined in 2 of the 4 controls (n=2). **E-G.** CD8$^+$ T cell numbers (F) numbers of CD8$^+$IFN-γ^+ and CD8$^+$Perforin$^+$ cells (H) and cytotoxicity of CD8$^+$ T cells (G) on day 21 post-stimulation of PBMCs from P1 with HLA-matched EBV-B cells and of normal PBMCs stimulated with autologous EBV-B cells without or with addition of anti-4-1BB blocking antibody BBK-2 (n=4 and n=2, respectively). We were able to study P1 CD8$^+$ T cell cytotoxicity against HLA-matched EBV-B cell targets once, because the patient underwent HSCT. Symbols and bars in B, D, E and G and columns and bars in C and F represent mean and SEM. *= p<0.05, ** p<0.01, *** p<0.001, ns= not significant.

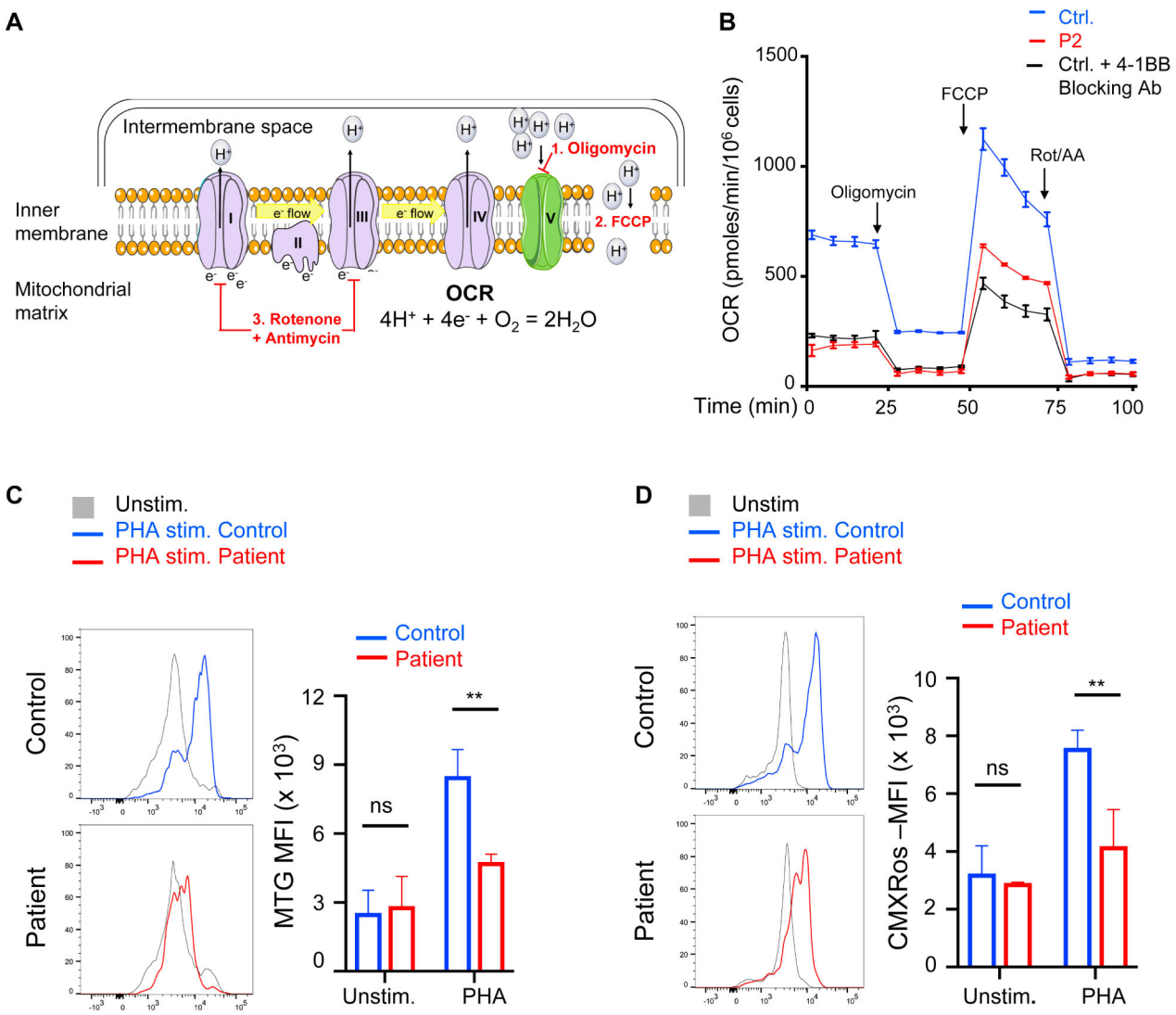

Figure 4. Defective mitochondrial biogenesis and function in the patients' activated CD8$^+$ T cells.

A. Schematic of factors determining the oxygen consumption rate (OCR). Complexes I – IV comprise the electron transport chain. The stepwise addition of reagents used during the extracellular flux analysis (1 – 3) are depicted in red. **B.** Extracellular flux analysis of T cells purified from PHA-stimulated PBMCs for 3 days from P2 (data pooled from two independent experiments) and controls without or with 4-1BB blocking antibody BBK-2 (n=2). **C, D**. Representative FACS analysis (left) and quantitative analysis (MFI, right) of mitochondrial mass measured using MitoTracker Green (MTG) (C) and of mitochondrial membrane potential measured using MitoTracker Red CMXRos (D) of CD8$^+$ cells in PHA stimulated cultures of PBMCs from patients (n=2) and controls (n=3). Columns and bars represent mean + SEM. ** $p<0.01$, ns= not significant.

Table 1.

Immunological profiles of the patients.

Hemogram (normal range)	**P1 5 years (Post Rituximab)**	**P2 9 years (Post Chemotherapy)**
Hemoglobin, g/dL	11.3 (10.5-13.8)	11.8 (11.9-14.7)
WBCs, 10^3 cells/μL	10.4 (5.4-9.7)	3.1 (4.4-9.1)
Neutrophils, 10^3 cells/μL	2.39 (1.5-5.9)	1.4 (1.8-8.0)
Lymphocytes, 10^3 cells/μL	6.81 (1.28-2.76)	0.96 (1.9-3.7)
Monocytes, 10^3 cells/μL	0.65 (0.19-0.81)	0.6 (<0.8)
Platelets, 10^3 cells/μL	412 (187-450)	196 (247-436)
Lymphocyte subsets (normal range)		
$CD3^+$, cells/μL	3352 (770-4000)	807 (1200-2600)
$CD3^+CD4^+$, 10^3 cells/μL	2766 (400-2500)	365 (650-1500)
$CD45RA^+CCR7^+$, % $CD4^+$ (Naïve)	23.9 (57.1-84.8)	8 (57.1-84.8)
$CD45RA^+CCR7^-$, % $CD4^+$ (Temra)	1.18 (0.4-2.6)	0.7 (0.4-2.6)
$CD45RA^-CCR7^+$, % $CD4^+$ (CM)	9.8 (11.2-26.7)	22.3 (11.2-26.7)
$CD45RA^-CCR7^-$, % $CD4^+$ (EM)	65.1 (3.3-15.2)	69.7 (3.3-15.2)
$CD3^+CD8^+$, cells/μL	627 (490-1300)	413 (370-1100)
$CD45RA^+CCR7^+$, % $CD8^+$ (Naïve)	42.4 (28.4-80)	17.8 (28.4-80
$CD45RA^+CCR7^-$, % $CD8^+$ (Temra)	7.36 (9.1-49.1)	29.8 (9.1-49.1)
$CD45RA^-CCR7^+$, % $CD8^+$ (CM)	0.7 (1- 4.5)	3.5 (1- 4.5)
$CD45RA^-CCR7^-$, % $CD8^+$ (EM)	49.6 (6.2-29.3)	48.9 (6.2-29.3)
$CD19^+$, cells/μL	0 (390-1400)	0 (270-860)
$CD3^-D56^+$, cells/μL	114 (110-720)	144 (80-600)
Proliferation CPM (normal control)		
PHA	64,562 (113,646)	56,218 (111,191)
Anti-CD3+Anti-CD28	20.650 (78,008)	35,638 (72,876)
Media	1,905 (1504)	195 (145)

ND, not done